PCCP

Electron transfer in nonpolar media

SCHOLARONE™
Manuscripts

ROYAL SOCIETY OF CHEMISTRY

Journal Name

ARTICLE TYPE

Electron transfer in nonpolar media[†]

Dmitry V. Matyushov[∗a]

The Marcus theory of electron transfer views fluctuating orientations of permanent dipoles as the nuclear mode bringing the donor and acceptor into the tunneling resonance. Electronic polarization of the solvent is excluded as the fast mode adiabatically following the electronic density. This view, valid for solids, does not apply to molecular liquids where molecular translations (density fluctuations) modulate the induction interaction of the donor-acceptor complex with the solvent. This mechanism of promoting radiationless electronic transitions is considered here in the framework of the perturbation liquid-state theory. The reorganization energy of electron transfer in nonpolar solvents is nonzero and reaches the values of 0.1–0.3 eV for typical molecular sizes and solvents used in applications. The reorganization energy scales quadratically with the molecular polarizability of the solvent and decays as the inverse fifth power with the size of the donor and acceptor. The combination of the entropic character of the density fluctuations, driven by re-packing of molecular cores, with the short range of induction solute-solvent interactions leads to the violation of the fluctuation-dissipation theorem for the variance of the donor-acceptor energy gap. An explicit, approximately hyperbolic, dependence of the reorganization energy on temperature is predicted. It leads to a non-Arrhenius kinetic law for the rate constant of electron transfer in nonpolar liquid solvents.

1 Introduction

The theory of electron transfer between electronic states localized on the donor and acceptor particles immersed in a polar medium was developed by Marcus.[1] In this model, activation of radiationless tunneling of the localized electron is driven by thermal agitation of the medium. A rare collective fluctuation of a large number of dipoles creates an electrostatic configuration in which the donor and acceptor electronic states come into resonance. This is the nuclear configuration in which tunneling of the electron becomes possible with the probability determined by the rules of quantum mechanics.

The fluctuating polar medium plays the role of the thermal bath modulating the difference of energies between the acceptor and donor electronic states, the donor-acceptor energy gap ΔE defined more precisely below. The energy gap becomes the collective reaction coordinate monitoring the progress of the reaction.[2–4] The reaction rate is proportional to the probability of achieving the tunneling configuration $\Delta E = 0$. Given a large number of medium's dipoles participating in the nonequilibrium fluctuation, the probability of this event is a Gaussian function specified by two parameters: the average energy gap $\langle \Delta E \rangle$ and the energy-gap variance σ^2. The probability of achieving $\Delta E = 0$ is then[5,6]

$$P(\Delta E = 0) \propto \exp\left[-\frac{\langle \Delta E \rangle^2}{2\sigma^2} \right]. \tag{1}$$

The next step of the theory is to express the energy-gap variance as the product of the thermal energy $k_{\mathrm{B}}T$ and the energy parameter λ known as the reorganization energy of electron transfer

$$\sigma^2 = \langle (\delta \Delta E)^2 \rangle = 2k_{\mathrm{B}}T\lambda, \quad \delta \Delta E = \Delta E - \langle \Delta E \rangle. \tag{2}$$

This form for the variance of ΔE is the static limit of the macroscopic fluctuation-dissipation theorem (FDT),[7,8] also known as the Johnson-Nyquist noise.[9] The FDT converts the probability $P(\Delta E = 0)$ into the Boltzmann distribution, with the rate constant of the reaction given by the Arrhenius kinetic law

$$k_{\mathrm{ET}} \propto P(\Delta E = 0) \propto e^{-\Delta F^\dagger/(k_{\mathrm{B}}T)}, \tag{3}$$

where

$$\Delta F^\dagger = \langle \Delta E \rangle^2 / (4\lambda) \tag{4}$$

is the activation free energy.

The FDT is formulated for an extensive, macroscopic variable A, which, when coupled to an intensive external conjugate force F, makes the perturbation $-A \times F$ to the extensive system Hamiltonian.[7] The prediction of the FDT then concerns the temperature scaling of the variance $\langle (\delta A)^2 \rangle \propto T$, which also scales linearly

[a] Department of Physics and School of Molecular Sciences, Arizona State University, PO Box 871504, Tempe, AZ 85287-1504; E-mail: dmitrym@asu.edu

with the number of particles in the system (an extensive parameter). On the contrary, variances of microscopic variables, which do not scale linearly with the number of particles, do not necessarily follow FDT's linear scaling $\sigma^2 \propto T$, thus leading to a number of violations of the FDT reported in the literature. [10–12]

Given that the donor-acceptor energy gap is a microscopic variable, deviations from the anticipated linear scaling with temperature [13] lead to experimentally detectable [14] deviations from the Arrhenius law. In contrast, the Marcus formulation for σ^2 applies the macroscopic FDT. It relies, in addition to the FDT, on the macroscopic dielectric susceptibility of a polarizable medium to calculate the reorganization energy λ. The Marcus theory is, therefore, a consistent macroscopic description of both the statistics of ΔE and the solvation thermodynamics. The question is to what extent the limitations of this picture, related to both the microscopic structure of the solute-solvent interface and to the microscopic character of the energy-gap collective variable, are reflected by the observables.

The Marcus reorganization energy $\lambda \propto c_0$ is proportional to the Pekar factor [15,16] $c_0 = \varepsilon_\infty^{-1} - \varepsilon_s^{-1}$, which originally appeared in theories of polarons in polar crystals. [15,17,18] It is defined in terms of the high-frequency, ε_∞, and static, ε_s, dielectric constants of a polarizable medium. This dielectric parameter arises from the difference of the longitudinal dielectric susceptibilities [19] $\chi^L = (4\pi)^{-1}(1 - \varepsilon_s^{-1})$ for the overall dielectric response and $\chi_\infty^L = (4\pi)^{-1}(1 - \varepsilon_\infty^{-1})$ for the electronic (high-frequency) component only: $c_0 = 4\pi \left[\chi^L - \chi_\infty^L \right]$. This form of the dielectric susceptibility appears in dielectric theories when an external source of charge with the spherically-symmetric electric field polarizes a spherically-symmetric cavity carved from the dielectric (Born theory of ion solvation [20]). This configuration, and the corresponding field symmetry, are not applicable to the majority of electron-transfer reactions in solutions. Extensions to more complex molecular shapes in the framework of dielectric theories produce more complex dielectric response functions combining both the longitudinal and transverse susceptibilities. [21] Nevertheless, if subtraction of the electronic response from the total is applied to construct the response of the nuclear polarization, all these functions carry the same mathematical form of a difference between overall and high-frequency susceptibilities. An alternative framework requires direct integration of the vector field of the electronic polarization in the free-energy functional [22–24] (eqn (9) below). This more precise approach yields non-additive forms of the response function, in which the electronic and overall susceptibilities are not separable anymore.

In a non-dipolar solvent, such as benzene or a hydrocarbon solvent, one gets $\varepsilon_s \approx \varepsilon_\infty$ and $c_0 \to 0$. From Marcus theory, one anticipates $\lambda \to 0$, which is an unphysical result (no thermal noise produced by the medium) contradicting the empirical evidence. Experiment suggests a substantial reorganization energy [25,26] $\lambda \simeq 0.1 - 0.3$ eV in non-dipolar materials, also measured through the Stokes shift of optical dyes. [27] To address the difficulty, the theory has to be re-formulated by departing from the realm of macroscopic dielectric polarization to microscopic liquid-state theories explicitly considering interactions of the donor-acceptor complex with molecular charges of the solvent. Describing non-dipolar

solvents requires incorporating either multipolar moments higher than the dipole (mostly quadrupole) [27–33] and/or molecular polarizability. [34–36]

The potential significance of molecular quadrupoles is easy to appreciate already within the conceptual framework of the Marcus theory. Nuclear motions, mostly rotations, of the molecular quadrupoles produce fluctuations of the electrostatic potential, [31] which are ultimately recorded by the donor-acceptor complex as changes in the donor-acceptor electronic energy gap. [27–30] Explicit relations for the reorganization energy following from this perspective are provided below.

On the other hand, significance of molecular polarizability, and of the corresponding electronic polarization, for electron transfer is harder to appreciate since it is exactly this polarization mode that is excluded from the solvent reorganization energy by the Marcus construction [1] leading to the Pekar factor. The reason for this exclusion is that electronic polarization is fast and follows the transferred electron adiabatically. This argument suggests that electronic polarization cannot be out of equilibrium with a given charge distribution of the solute. It, therefore, needs to be subtracted from the total medium polarization to arrive at the nuclear polarization of the medium, which is capable of deviating from equilibrium due to thermal agitation. This logic leads to the Pekar factor when applied to the longitudinal polarization of the medium.

These arguments, going back to the theory of polarons in solid materials, [15,17,18] are obviously correct. However, they are focused on orientational fluctuations of dipoles in a solid-type medium and miss the importance of molecular translations in producing nuclear fluctuations in molecular liquids. [37,38] We first briefly discuss the conceptual steps of the theory incorporating these nuclear modes, [34,35] followed by the full formalism.

One starts with solving the eigenvalue problem for a molecule in the gas phase by standard quantum mechanical algorithms. This step provides eigenenergies E_{gi} and multielectron eigenstates ϕ_i, $i = 1, 2$. In the next step, the molecule is placed in the medium and the molecule-medium interaction is added to the gas-phase Hamiltonian H_g

$$H = H_g - \int d\mathbf{r} \hat{\mathbf{E}}_0 \cdot \mathbf{P}. \tag{5}$$

Here, $\hat{\mathbf{E}}_0$ is the operator of the electric field of the donor-acceptor complex and $\mathbf{P}$ is the polarization density of the medium. In the first order of the perturbation theory, the energy $E_i = \langle \phi_i | H | \phi_i \rangle$ is shifted from E_{gi} by the interaction

$$-\int d\mathbf{r} \mathbf{E}_{0i} \cdot \mathbf{P} \tag{6}$$

of the electric field $\mathbf{E}_{0i} = \langle \phi_i | \hat{\mathbf{E}}_0 | \phi_i \rangle$ in the state ϕ_i with the polarization field

$$\mathbf{P} = \mathbf{P}_n + \mathbf{P}_e. \tag{7}$$

The latter includes both the nuclear component $\mathbf{P}_n$ from reorientations of molecular multipoles and the electronic component $\mathbf{P}_e$ from induced (electronic) molecular dipoles. Note that $\mathbf{P}_n = \mathbf{P}_d - \frac{1}{3} \nabla \cdot \mathbf{Q} + \dots$ formally includes [39] the vector field of dipolar density $\mathbf{P}_d$, as well as densities of higher multipoles, such as

the most important for non-dipolar solvents [28–32,40] quadrupolar density $\mathbf{Q}$ (a second-rank tensor field).

The first-order quantum-mechanical perturbation theory yields instantaneous energies of the donor and acceptor $H_i[\mathbf{P}_e, \mathbf{P}_n]$ fluctuating due to thermal fluctuations of two vector fields, $\mathbf{P}_e$ and $\mathbf{P}_n$

$$H_i[\mathbf{P}_e, \mathbf{P}_n] = E_{gi} - \int d\mathbf{r} \mathbf{E}_{0i} \cdot \mathbf{P} \qquad (8)$$

For the rest of our study, we will drop the nuclear polarization and focus only on the electronic polarization $\mathbf{P}_e$. Therefore, we put $\mathbf{P}_n = 0$ in eqn (7) and (8).

The next step of the theory is to adiabatically exclude the fast electronic polarization of the medium. [41] This is achieved by taking the trace of the density matrix $\hat{\rho}_i = \exp(-\beta H_i[\mathbf{P}_e])$, $\beta = 1/(k_B T)$ over the fast quantum field $\mathbf{P}_e$

$$e^{-\beta E_i} = \mathrm{Tr}_e[\hat{\rho}_i]. \qquad (9)$$

Depending on the form of the functional $H_i[\mathbf{P}_e, \mathbf{P}_n]$ and the details of interactions between the induced and permanent dipoles, eqn (9) leads, in the continuum limit, to either the Pekar factor for the nuclear susceptibility or to alternative relations accounting for the effect of the electronic polarization in a nonadditive fashion. [24]

Electronic tunneling occurs between the energy levels E_i adiabatically dressed by the electronic polarization of the medium. They are brought into resonance $\Delta E = 0$ by thermal modulation of the energy gap defined by the equation

$$\Delta E = E_2 - E_1 \qquad (10)$$

with E_i from eqn (9). The goal of this study is to develop a quantitative model for the free energy barrier required to achieve the resonance state. We focus on arriving at closed-form expressions applicable to interpreting experiment.

In addition to the fundamental framework of describing activated electronic transitions in low-polarity media, there is a practical dimension to the present theoretical development. Current interest in electron-transfer reactions in nonpolar media [25,42–45] is driven by applications of photoinduced electron transfer to solar energy conversion. [25] Charge separation in a low-polarity medium can serve as a generic model for charge separation in organic photovoltaic cells. Low-polarity solvents produce a lower solvation free energy for the charge-separated state, thus requiring a lower driving force to achieve the near-activationless electronic transition with $\langle \Delta E \rangle \approx 0$ in eqn (1). The driving force is the negative of the reaction free energy, $-\Delta F_0$, which, in the Marcus theory, [1] combines with the reorganization energy λ to make the average vertical energy gap

$$\langle \Delta E \rangle_i = \Delta F_0 \pm \lambda. \qquad (11)$$

Here, for the energy gap defined by eqn (10), $+$ and $-$ correspond to the forward, $i = 1$ in the average $\langle \ldots \rangle_i$, and backward, $i = 2$, reactions, respectively. The condition $-\Delta F_0 = \lambda$ specifies zero activation barrier for the forward reaction, when the rate is maximized. Lower λ implies lower driving force $-\Delta F_0$ required to maximize the rate. For charge (hole and electron) conductivity

in organic semiconductors, [46] a lower solvation energy implies a lower level of disorder and a lower trapping energy for the charge carrier. [25]

The model presented here looks for a formulation involving a minimal number of well defined parameters to calculate $\langle \Delta E \rangle_i$ and λ arising from induction interactions between the solute and a polarizable non-dipolar solvent. The liquid solvent is reduced here to an effective medium of polarizable molecules fluctuating as determined by the density structure factor. The latter can be measured by neutron and x-ray scattering and calculated from liquid-state theories and numerical simulations. [8,47,48] Even though this input can be used in a detailed formalism presented below, this information is hard to gain for most molecular solvents and further reduction of the model is required. It is achieved by introducing a simplified approximation for the reciprocal-space integral of the solute-solvent interaction with the density structure factor. The final minimalist model, which is tested against computer simulations, arrives at the solution for the induction reorganization energy in terms of liquid's high-frequency dielectric constant (squared refractive index), its density, and molecular sizes of the solvent and solute molecules.

2 Induction interactions

Integration over the Gaussian vector field $\mathbf{P}_e$ in eqn (9) adds the free energy of electronic solvation to the gas-phase energy E_{gi}

$$F_{ei} = -\tfrac{1}{2} \int d\mathbf{r} \mathbf{E}_{0i} \cdot \langle \mathbf{P}_e \rangle_i. \qquad (12)$$

The electronic polarization $\langle \mathbf{P}_e \rangle_i$ in this equation represents induced electronic dipoles at the molecules of the medium in equilibrium (specified through $\langle \ldots \rangle_i$) with the vacuum electric field $\mathbf{E}_{0i}$. This free energy is usually viewed to represent the equilibrium nuclear configuration of the liquid, but it does not need to. Since this is a partial free energy allowing the nuclear coordinates to change (in other words, a potential of mean force), positions of the induced molecular dipoles can fluctuate due to thermal agitation (density fluctuations [13,38]). As a result, the partial free energy F_{ei} will fluctuate as well.

This point becomes particularly clear when the electronic free energy F_{ei} is re-written in terms of separate molecular induced dipoles specified by the isotropic molecular polarizability α

$$F_{ei} = -(\alpha/2) \sum_j \mathbf{E}_{0i}^2(j). \qquad (13)$$

Here, $\mathbf{E}_{0i}(j)$ is the electric field of the donor-acceptor complex at the position of molecule j and the sum runs over the solvent molecules. It is clear from this expression that collective fluctuations of the positions of the molecules will produce corresponding fluctuations of the partial free energies F_{ei} and of the instantaneous energies $E_i = E_{gi} + F_{ei}$ between which the electron tunnels.

One next proceeds to define the energy-gap reaction coordinate [3,49,50]

$$X = E_2 - E_1 = \Delta E_g + \Delta F_e \qquad (14)$$

monitoring the progress of the reaction to the point of the tunneling configuration (transitions state) at $X = 0$. Here, $\Delta E_g =$

$E_{g2} - E_{g1}$ is the gas-phase vertical energy gap at the molecular geometry of the donor-acceptor complex in the initial state from which electron transfer occurs. Further, ΔF_e is the solvent-induced shift of the vertical energy gap due to the solute-solvent induction interaction.

The average solvent-induced shift can be found from the first-order perturbation theory [8,51,52] as

$$\langle \Delta F_e \rangle_i = \langle \Delta F_e \rangle - \beta \langle \delta X \delta F_{ei} \rangle. \tag{15}$$

Here, the average $\langle \ldots \rangle_i$ includes the solute-solvent interaction F_{ei} in the system Hamiltonian, while the statistical average $\langle \ldots \rangle$ does not include this term. Therefore, $\langle \ldots \rangle$ is the statistical average over the configurations of the solvent and the solute specified by all interactions in the solvent and the solute-solvent interactions excluding the induction solute-solvent component.

From eqn (15), one obtains for the difference between equilibrium energy gap values (the Stokes shift [27])

$$\langle X \rangle_1 - \langle X \rangle_2 = \beta \langle (\delta X)^2 \rangle = 2\lambda, \tag{16}$$

where the reorganization energy λ is defined by eqn (2). One also finds from eqn (11) and (15)

$$\Delta F_0 = \frac{1}{2} \left(\langle X \rangle_1 + \langle X \rangle_2 \right). \tag{17}$$

If FDT ($\sigma^2 \propto T$) is applied to the variance $\sigma^2 = \langle (\delta X)^2 \rangle$ in eqn (16), the reorganization energy λ does not carry any explicit dependence on temperature (it depends on temperature through other parameters, such as the liquid density ρ). However, σ^2 does not have to follow the macroscopic FDT and, indeed, its temperature dependence is more complex even in the case of polar liquids when the macroscopic theory of medium polarization is replaced with a microscopic description. [13] When molecular translations are allowed for the solvent dipoles (density fluctuations), [37] the corresponding density component of the reorganization energy gains $\propto T^{-1}$ temperature scaling. [13,14,38] This is an observable consequence of the short-ranged character of the density fluctuations mostly driven by rearrangement of molecular repulsive cores (an entropic packing effect). The overall dependence of the energy-gap variance on temperature is linear (at constant ρ), $\sigma^2 = a + bT$, with a non-zero $T = 0$ intercept caused by the density fluctuations. [13]

Given that the interaction of the charge with the induced dipole is more short-ranged, $\propto r^{-4}$, than the interaction of the charge with the permanent dipole, $\propto r^{-2}$, the strict linear temperature law for the variance should not be anticipated (fewer particles participate in creating the reactive fluctuation). Indeed we show below that σ^2 remains constant when the macroscopic density of the liquid is kept unchanged. This result projects into the reorganization energy inversely proportional to temperature, $\propto T^{-1}$, unlike the nearly constant reorganization energy $\lambda \propto c_0$ in dielectric theories describing dipolar orientational fluctuations. Since induction forces are universal for all solvents, the induction reorganization energy adds to the density fluctuations of the permanent dipoles in the overall linear temperature scaling of the energy-gap variance, $\sigma^2 = a' + bT$, with a' accounting for the density fluctuations translating both permanent and induced dipoles.

Equations (16) and (17) indicate that the problem at hand is the standard Marcus picture of two shifted parabolas with their minima separated by 2λ and the curvatures given as $(2\lambda)^{-1}$. The average energy gap $\langle \Delta E \rangle_i$ entering the Gaussian probability in eqn (1) contains the reaction free energy ΔF_0 according to eqn (11). As mentioned above, solvent multipoles are neglected altogether here and the focus is solely on molecular polarizability. This approach applies to either non-dipolar solvents with small quadrupole moments or to solvents where quadrupole is zero by symmetry (such as CCl_4). Since polarizability is a universal property shared by all molecules, the present model provides the lower bound to the reorganization energy in non-dipolar solvents.

3 Formalism

Following the arguments presented above, the solvent-induced shift of the vertical energy gap is given as follows [34–36]

$$\Delta F_e = \sum_j v(j) = -(\alpha/2) \sum_j \left[E_{02}(j)^2 - E_{01}(j)^2 \right]. \tag{18}$$

The solute-solvent interaction can be written as the integral over the microscopic fluctuating density $\rho(\mathbf{r})$

$$\Delta F_e = \int d\mathbf{r} v(\mathbf{r}) \rho(\mathbf{r}), \quad \rho(\mathbf{r}) = \sum_j \delta \left(\mathbf{r} - \mathbf{r}_j \right). \tag{19}$$

Therefore, the second moment of $\delta X = \delta \Delta F_e$ is given as

$$\langle (\delta X)^2 \rangle = \int d\mathbf{r}_1 d\mathbf{r}_2 v(\mathbf{r}_1) v(\mathbf{r}_2) \langle \delta \rho(\mathbf{r}_1) \delta \rho(\mathbf{r}_2) \rangle. \tag{20}$$

In this equation, the density-density correlation function $\langle \delta \rho(\mathbf{r}_1) \delta \rho(\mathbf{r}_2) \rangle$ can be written [8] in terms of single-particle density profiles around the solutes $\rho^{(1)}(\mathbf{r}) = \langle \rho(\mathbf{r}) \rangle$ and of the two-particle (pair) density $\rho^{(2)}(\mathbf{r}_1, \mathbf{r}_2)$

$$\langle \delta \rho(\mathbf{r}_1) \delta \rho(\mathbf{r}_2) \rangle = \rho^{(1)}(\mathbf{r}_1) \delta(\mathbf{r}_1 - \mathbf{r}_2) + \rho^{(2)}(\mathbf{r}_1, \mathbf{r}_2) - \rho^{(1)}(\mathbf{r}_1) \rho^{(1)}(\mathbf{r}_2)$$

$$= \rho^{(1)}(\mathbf{r}_1) \delta(\mathbf{r}_1 - \mathbf{r}_2) + \rho^{(1)}(\mathbf{r}_1) \rho^{(1)}(\mathbf{r}_2) h(\mathbf{r}_1, \mathbf{r}_2), \tag{21}$$

where $h(\mathbf{r}_1, \mathbf{r}_2)$ is the pair correlation function (eqn (3.1.6) in Ref. 8).

The correlation function $h(\mathbf{r}_1, \mathbf{r}_2)$ describes the joint probability to find two solvent particles at $\mathbf{r}_1$ and $\mathbf{r}_2$ in the inhomogeneous liquid perturbed by solute's repulsive core. The approximation often applied in problems of solvation [34,35,53–56] and adopted here is to replace the inhomogeneous correlation function $h(\mathbf{r}_1, \mathbf{r}_2)$ with the correlation function $h_{ss}(r_{12})$, $\mathbf{r}_{12} = \mathbf{r}_2 - \mathbf{r}_1$ of the homogeneous bulk liquid. The variance of this energy gap can then be written in terms of the solute-solvent pair distribution function $g_{0s}(r)$, $\rho^{(1)}(\mathbf{r}) = \rho g_{0s}(\mathbf{r})$ and of the solvent-solvent correlation function $h_{ss}(r_{12})$ as follows

$$\langle (\delta X)^2 \rangle = \rho \int d\mathbf{r}_1 g_{0s}(r_1) v(\mathbf{r}_1)^2$$

$$+ \rho^2 \int d\mathbf{r}_1 d\mathbf{r}_2 g_{0s}(r_1) v(\mathbf{r}_1) g_{0s}(r_2) v(\mathbf{r}_2) h_{ss}(r_{12}), \tag{22}$$

where $\rho = N/V$ is the number density for N solvent molecules occupying the volume V.

The next goal is to arrive at a representation of the energy-gap variance in eqn (22) in terms of the structure factor of the density fluctuations of the liquid for the reason that will become clear immediately. The difficulty here is that the solute-solvent pair distribution function $g_{0s}(r)$ enters the first summand in eqn (22) in the first order, while it enters the second summand in the second order. To avoid this difficulty, one can define an effective solute-solvent interaction [29]

$$u(r) = g_{0s}^{1/2}(r)v(r), \qquad (23)$$

which allows us to approximate eqn (22) in reciprocal space as

$$\langle(\delta X)^2\rangle = \rho \int \frac{d\mathbf{k}}{(2\pi)^3} S(k)u(\mathbf{k})^2, \qquad (24)$$

where $u(\mathbf{k})$ is the Fourier transform of the effective potential in eqn (23) and $S(k) = 1 + \rho h_{ss}(k)$ is the density-density structure factor of the bulk solvent. [8] Its $k = 0$ value is related to the solvent isothermal compressibility β_T

$$S(0) = k_B T \rho \beta_T. \qquad (25)$$

The opposite limit of $k \to \infty$ gives $S(k) \to 1$.

One can next use eqn (2) to write the reorganization energy of induction interactions in the following form

$$\lambda^{\text{ind}} = \frac{9e^4 \beta_T}{\sigma_s^5} \left(\frac{\varepsilon_\infty - 1}{\varepsilon_\infty + 2}\right)^2 g^{\text{ind}}, \qquad (26)$$

where we have indicated (subscript "ind") the origin of the reorganization energy from induction solute-solvent interaction, e is the elementary charge, and σ_s is the solvent molecular diameter. The high-frequency dielectric constant ε_∞, which for most applications can be identified with the squared refractive index, appears in eqn (26) through the Clausius-Mossotti relation [57]

$$\frac{\varepsilon_\infty - 1}{\varepsilon_\infty + 2} = \frac{4\pi}{3}\rho\alpha. \qquad (27)$$

Equation (26) thus implies that λ^{ind} scales quadratically with the solvent molecular polarizability α.

The last term, g^{ind}, in eqn (26) reflects the geometry of the donor-acceptor complex and the solute-solvent density profile. It is given by the reciprocal-space integral

$$g^{\text{ind}} = \int_0^\infty F(k)\tilde{S}(k)dk. \qquad (28)$$

Here,

$$F(k) = \sigma_s^5(k^2/(4e\pi)^4)\langle\left|(E_{02}^2)_\mathbf{k} - (E_{01}^2)_\mathbf{k}\right|^2\rangle_{\hat{\mathbf{k}}} \qquad (29)$$

and $(E_{0i}^2)_\mathbf{k}$ is the space Fourier transform of the product of $E_{0i}(\mathbf{r})^2$ with $g_{0s}^{1/2}(\mathbf{r})$

$$(E_{0i}^2)_\mathbf{k} = \int_\Omega d\mathbf{r}E_{0i}^2(\mathbf{r})g_{0s}^{1/2}(\mathbf{r})e^{i\mathbf{k}\cdot\mathbf{r}}. \qquad (30)$$

The integral is taken outside of the repulsive core of the donor-acceptor complex and over the volume Ω occupied by the solvent; $\langle\ldots\rangle_{\hat{\mathbf{k}}}$ in eqn (29) is the average over the directions of the wavevector $\hat{\mathbf{k}} = \mathbf{k}/k$.

The scaled structure factor $\tilde{S}(k) = S(k)/S(0)$ in eqn (28) takes $S(0)$ (eqn (25)) in front of the k-integral. This representation is the reason for both the cancellation of $k_B T$ from the definition of the reorganization energy in eqn (2) and (16) and the appearance of the isothermal compressibility β_T in the equation for λ^{ind}. This definition of λ^{ind} is motivated by the analogous formulation for the reorganization energy due to dipolar polarization, where the $k = 0$ limit of the longitudinal structure factor $S^L(0)$ produces the dominant contribution to the k-integral. [38] Since putting $S^L(k) \simeq S^L(0)$ in the definition of the reorganization energy in terms of the corresponding k-integral yields the continuum result for the reorganization energy in a dipolar liquid, the success of this approximation is responsible for the success of dielectric theories in describing polar solvation.

The continuum limit, $S^L(k) \approx S^L(0)$, for the fluctuations of molecular permanent dipoles is a reasonable first-order approximation since the reciprocal-space integral in that case is dominated by the values of wavevector close to $k = 0$, where $S^L(k)$ is relatively flat (in contrast to the transverse structure factor $S^T(k)$ [21]). In other words, due to the long-ranged, [58,59] $\propto r^{-3}$, character of angular correlations between the liquid dipoles, the macroscopic FDT, with a temperature-independent (at constant density) λ, is a reasonable approximation for fluctuations arising from dipolar rotations. It fails, however, for dipolar translations. [38]

The question addressed here is whether the picture of macroscopic fluctuations used to describe reorganization by permanent dipoles applies to reorganization by induced dipoles. In mathematical terms, this question is equivalent to asking whether the continuum limit $k \approx 0$ mostly contributes to the integral in eqn (28). If, on the contrary, large values of k substantially contribute to the integral, the absence of an explicit dependence on temperature in eqn (26) might be a poor representation of the physics of short-ranged induction interactions modulated by the thermal noise. Answering this question is best achieved within an analytical framework, when the integrals involved can be integrated to closed-formed expressions, with both the microscopic and macroscopic limits following from the same formalism. We, therefore, consider the half redox reaction [6] of electron transfer to a spherical particle (Fig. 1) as a model for electron transfer in an electrochemical setup and for solvation of ions in nonpolar solvents. [60] We indeed find that the $k \to 0$ limit is a poor representation for the integral in eqn (28), which physically means that the response of induced dipoles is local and short-ranged. As a result, we find $\lambda^{\text{ind}} \propto 1/T$ for the induction reorganization energy. The corresponding energy-gap variance σ^2 turns out to be nearly constant when temperature is varied. The expectations of the FDT are not realized for reorganization of induced dipoles.

4 One-sphere geometry

Consider electron transfer to a single spherical particle changing its charge from ze in the initial ($i = 1$, oxidized) state to $(z-1)e$ in the final ($i = 2$, reduced) state (Fig. 1). This process corresponds
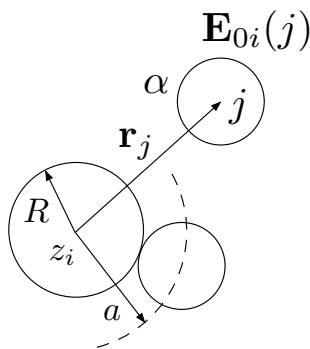
Fig. 1 One-sphere configuration of the solute carrying the charge $z_1 = z$ in the oxidized state and $z_2 = z - 1$ in the reduced state (eqn (31)); e is the elementary charge. The solute produces the electric field $\mathbf{E}_{0i}(j)$ at molecule j with the polarizability α. The induction free energy is $-(\alpha/2)\mathbf{E}_{0i}^2(j)$. The solute is viewed as a spherical particle with the radius R; $a = R + \sigma_s/2$ is the distance of the closest approach of the solvent molecule, where σ_s is the solvent hard-sphere diameter.

to the following half redox reaction

$$A^z + e^- \longrightarrow A^{z-1}. \tag{31}$$

The charge of the particle is the sole source of the electric field polarizing the surrounding nonpolar liquid. This simplified representation applies to electrode half reactions when the field of the image charges in the electrode can be neglected. It also applies to solvation of ions in nonpolar solvents and to trapping energy of the conduction polaron in conducting conjugated polymers dissolved in nonpolar solvents. [61]

In the one-sphere geometry, the instantaneous induction interaction in eqn (18) becomes

$$\Delta F_e = (2z - 1)V, \quad V = \sum_j \frac{\alpha e^2}{2r_j^4}. \tag{32}$$

The ensemble average in the state with the charge z_i at the solute follows from eqn (15)

$$\langle \Delta F_e \rangle_i = (2z - 1)\langle V \rangle + \frac{2z_i^2}{2z - 1}\lambda^{\text{ind}}. \tag{33}$$

The ensemble average $\langle \ldots \rangle_i$ involves the solvent structure altered by the solute-solvent induction interactions. This effect is accounted for in eqn (33) by the perturbation theory of liquids [52] in terms of the solute-solvent induction interaction. This perturbation theory is also a part of the standard linear-response formulation of the electron-transfer theory, [38] which requires that λ does not dependent of the redox state. It should, therefore, be calculated in zeroth order in the interaction potential altered by charge transfer, [6] which is the induction solute-solvent interaction here. This implies that the subscript can be dropped from $\langle \ldots \rangle_i$ in the definition of the reorganization energy (eqn (16) and (22))

$$\beta\lambda^{\text{ind}} = \tfrac{1}{2}(2z - 1)^2 \langle (\beta\delta V)^2 \rangle. \tag{34}$$

This equation was used to specify the second term in eqn (33).

The one-sphere model allows us to analyze the principle pa-

rameters affecting electron transfer in nonpolar liquids since the function $F(k)$ in eqn (28) and (29) is now well-defined. Considering more complex geometries requires numerical Fourier transform to calculate $F(k)$ in eqn (29). For one-sphere geometry, one has

$$F(k) = \frac{(2z - 1)^2 \sigma_s^5}{(4\pi)^2} f_3^2(k, a), \tag{35}$$

where

$$f_n(k, a) = \int_a^\infty \frac{dr}{r^n} g_{0s}^{1/2}(r) \sin(kr) \tag{36}$$

Further, in eqn (35)

$$a = R + \sigma_s/2 \tag{37}$$

is the radius of the solvent-excluded sphere around the solute (Fig. 1).

One can first assume the continuum approximation, $\tilde{S}(k) = 1$, to hold in eqn (28). In this case, one arrives at the closed-form expression in eqn (26) with the following geometric factor

$$g^{\text{ind}} = \frac{(2z - 1)^2}{160\pi} \left(\frac{\sigma_s}{a_{\text{eff}}} \right)^5. \tag{38}$$

Here, the effective solute radius a_{eff} is given as

$$a_{\text{eff}}^{-5} = 5 \int_0^\infty (dr/r^6) g_{0s}(r). \tag{39}$$

This integral was tabulated as a polynomial form of $1/a$ and the reduced solvent density $\rho^* = \rho\sigma_s^3$ in Ref. 30. It is given for completeness in the ESI.[†] In the specific limit of $\rho^* \to 0$, when the density structure of the solvent around the solute disappears, one gets $a_{\text{eff}} \to a$. This is the limit when the solute-solvent radial distribution function is approximated by a step function

$$g_{0s}(r) \simeq \theta(r - a), \tag{40}$$

where $\theta(x)$ is the Heaviside function. Combined with eqn (26), the reorganization energy $\lambda^{\text{ind}} \propto (e^2/a)^2/(K_T a^3)$ becomes proportional to the ratio of the squared Coulomb energy e^2/a and the elastic energy $K_T a^3$, with $K_T = \beta_T^{-1}$ being the isothermal bulk modulus. In other words, this continuum limit suggests that an incompressible medium does not allow induction reorganization.

One can alternatively assume the opposite limit of large k-values, when $S(k) \to 1$, dominates in the k-integral in eqn (28). Physically, this assumption implies that microscopic fluctuation at the lengthscale comparable to the size of the solvent molecule are more important in affecting the solvent reorganization energy than the macroscopic compressibility of the medium. In this limit, $\tilde{S}(k) \approx S(0)^{-1}$ and one obtains $g^{\text{ind}} \to g^{\text{ind}} S(0)^{-1}$. Since $S(0) \ll 1$ for dense liquids, this microscopic limit obviously makes the reorganization energy much higher than in the continuum limit.

A continuous transition between the two limits can be achieved by taking $S(k)$ in an analytical form allowing k-integration in eqn (28). One can apply the Padé form [38] interpolating between the $k = 0$ and $k \to \infty$ limits

$$S(k) = \frac{S(0) + \Lambda^2 k^2}{1 + \Lambda^2 k^2}. \tag{41}$$

In the Percus-Yevick (PY) solution for $S(k)$, [8,52] the correlation

length of the density fluctuations is $\Lambda = 3\eta\sigma_s/(2+4\eta)$;[38] $\eta = (\pi/6)\rho\sigma_s^3$ is the packing fraction of the solvent. Adopting this form in the k-integral in eqn (28), one obtains

$$g^{ind} = \frac{(2z-1)^2\sigma_s^5}{160\pi S(0)}\left[a_{eff}^{-5} + (S(0)-1)G\right], \qquad (42)$$

where

$$G = \frac{5}{2\Lambda}\int_a^\infty \frac{dr'}{r'^3}g_{0s}^{1/2}(r')\int_a^\infty \frac{dr''}{r''^3}g_{0s}^{1/2}(r'')e^{-|r'-r''|/\Lambda}. \qquad (43)$$

If the correlation length of the density fluctuations is significantly shorter than the size of the solute a_{eff}, one can put $(2\Lambda)^{-1}\exp[-|r'-r''|/\Lambda] \simeq \delta(r'-r'')$ in eqn (43), with the result $G = a_{eff}^{-5}$. One then obtains the continuum limit for g^{ind} given by eqn (38). This derivation shows that the reorganization energy with no explicit dependence on temperature, as predicted by the FDT, can indeed be obtained for sufficiently large solutes. We now show that this limit is not reached when the size of the solute is comparable with the size of the solvent and, instead, the high-k limit $S(k) \to 1$ is a better approximation.

The integral in eqn (28) can be evaluated numerically with $S(k)$ provided by either numerical simulations or liquid-state theories. We adopt here a more direct route to calculating λ^{ind} by applying the PY solution for the density structure factor.[8,52] It is shown in the ESI† that this approach provides results comparable with the use of the structure factors from simulations of Lennard-Jones (LJ) liquids provided that the $k = 0$ value of the PY structure factor is adjusted to $S(0)$ of the LJ liquid. This is achieved by altering the packing fraction η of the HS liquid to match the condition $S(0) = S_{PY}(0)$, where [52]

$$S_{PY}(0) = (1-\eta)^4/(1+2\eta)^2. \qquad (44)$$

Since the density structure factors are not available for most nonpolar solvents of practical interest, we adopt this approach as a practical means to calculate the induction reorganization energy in molecular solvents. Specifically, we use the PY structure factor with the packing fraction adjusted to make $S_{PY}(0)$ in eqn (44) equal to the experimental $S(0)$ determined by the isothermal compressibility through eqn (25). The result of this approach is presented in Fig. 2 for a solvent with parameters of CCl$_4$ ($\sigma_s = 5.54$ Å, $\eta = 0.511$,[62] $\alpha = 11.2$ Å³,[52] $\beta_T = 10.94$ GPa^{-1}, and $\varepsilon_\infty = 2.1$) and the solute radius $R = 3$ Å. The packing fraction becomes equal to $\eta = 0.453$ when eqn (44) is applied to the experimental isothermal compressibility.

To simplify these illustrative calculations, $g_{0s}(r)$ is taken as a step function with the radius $a = R + \sigma_s/2$ (eqn (40)). We find that the continuum limit (eqn (38)) underestimates the numerical results by a factor of $\simeq 13$, while the result based on the $k \to \infty$ asymptote of the structure factor $S(k) \to 1$ overestimates the numerical result by a factor of $\simeq 3$. Therefore, in order to preserve the simple form of the final equations, an empirical factor κ was introduced to the equation for the induction reorganization energy

$$\lambda^{ind} = \frac{3\beta e^4(2z-1)^2}{320\eta}\kappa\left(\frac{\varepsilon_\infty - 1}{\varepsilon_\infty + 2}\right)^2\frac{\sigma_s^3}{a^5}. \qquad (45)$$
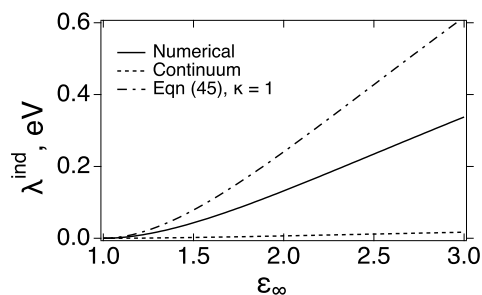

Fig. 2 Induction reorganization energy λ^{ind} vs ε_∞ for a model one-sphere solute with $R = 3.0$ Å. Calculations are performed for a liquid with properties of CCl$_4$ ($\sigma_s = 5.54$ Å[62]) and changing ε_∞ (polarizability). The solid line indicates direct numerical integration in eqn (28) with the Percus-Yevick density-density structure factor[8] and a step-function $g_{0s}(r)$ (eqn (40)). The continuum limit $S(k) \to S(0)$ in eqn (38) is shown by the dotted line. The dash-dotted line refers to eqn (45) with $\kappa = 1$. Equation (45) is brought in agreement with the numerical integration by adopting $\kappa = 0.31$.

We find that $\kappa = 0.31$ brings the analytical result into agreement with the numerical integration. This result corresponds to adopting $S(k) = \kappa$ in the k-integral. The value of κ is also fairly insensitive to the strength of attraction ε_{LJ} in the LJ liquid used in the simulations presented below: when $S(k)$ from simulations are directly used in eqn (28), κ changes from 0.3 to 0.27 in the range $\beta\varepsilon_{LJ} = 0.125 - 2.0$ (see ESI†).

A complete solution of the problem allowing a continuous transition between the microscopic and continuum limits requires direct account for the spatial correlations affecting density fluctuations in molecular liquids, such as those introduced through the Padé form for $S(k)$ in eqn (41). Our goal here is to avoid these complications and arrive at a practical solution applicable to interpreting experiment. Since an empirical correction parameter κ has been already introduced to account for the neglect of spatial density correlations, we have also adopted $a_{eff} \to a$ in eq (45). Direct numerical simulations of nonpolar polarizable fluids presented below support the analytical form for the reorganization energy given by eqn (45).

The main result of the calculations presented in Fig. 2 is the realization that, in contrast to electrostatics of dipolar liquids, the continuum limit is a poor representation for the fluctuations of induction interactions. Adopting the $k \to \infty$ limit for the structure factor overestimates the result, but turns out to be a much better representation of the numerical integral involving the full functional form of $S(k)$. The qualitative outcome is the appearance of a hyperbolic $\propto T^{-1}$ temperature dependence of the reorganization energy[34,35] as a general signature of short-ranged microscopic fluctuations violating the FDT.[13]

The reorganization energy λ^{ind} is found to scale with the inverse fifth power of the solute size, in contrast to the inverse first power for solvation by permanent dipoles. Therefore, when considering fixed solvent size and increasing solute size, induction reorganization can be significant only for sufficiently small solutes or for charges located close to the surface of large solutes. The solute charge is placed at the center of a spherical solute in the
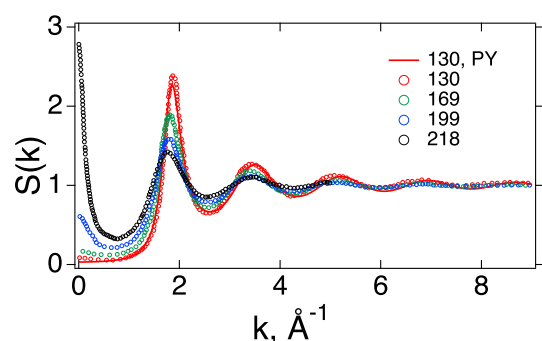
Fig. 3 $S(k)$ for Kr at $T = 130$ K ($\rho^* = 0.81$), 169 K ($\rho^* = 0.70$), 199 K ($\rho^* = 0.54$), and 218.18 K ($\rho^* = 0.45$) from neutron diffraction (points);[65,66] $\rho^* = \rho\sigma_s^3$. The solid line indicates the Percus-Yevick[8,52] (PY) structure factor $S_{PY}(k)$ calculated with the density at $T = 130$ K and $\sigma_s = 3.63$ Å.[64] The Lennard-Jones energy for Kr, $\varepsilon_{LJ}/k_B = 180$ K,[67] defines the energy scale of solvent-solvent attractions.

Table 1 Induction reorganization energies in Kr calculated from experimental density structure factors[65,66] assuming $a_{eff} = a = R + \sigma_s/2$, $R = 3$ Å (eqn (40)).

T, K	ρ^*	β_T, 10^{-10} Pa^{-1}	λ^{ind}, eV
130	0.81	21.6	0.024
169	0.70	52.1	0.020
199	0.54	237.5	0.021
218.18	0.45	988.1	0.030

present calculations. However, what really matters for the magnitude of the reorganization energy is the distance between the centroid of the electronic density and the polarizable medium.

The PY structure factor $S_{PY}(k)$ for a hard-sphere fluid gives a reasonable account of the structure of a dense liquid (Fig. 3), which is mostly affected by packing of the molecular repulsive cores[63] (also see Fig. S1 in ESI†). It is potentially less reliable for modeling temperature effects on the density fluctuations. However, in a narrow range of temperatures, one can approximate the temperature dependence of $S(0)$ by eqn (44) in which the packing fraction $\eta(T)$ is given in terms of the isobaric expansivity α_p. This calculation (Fig. S3 in ESI†) of $\lambda^{ind}(T)$ shows that $\lambda^{ind} \propto T^{-1}$ holds very well for both the full k-integration and for the simplified result given by eqn (45).

To assess the effect of temperature on λ^{ind} for more realistic conditions, we used the structure factors for krypton ($\alpha = 2.484$ Å^3,[52] $\sigma_s = 3.63$ Å[64]) measured by neutron diffraction at $T = 130$, 169, 199, and 218.18 K.[65,66] The structure factors $S(k)$ are shown in Fig. 3, and the results of integration with the experimental input in eqn (28) are listed in Table 1. We note that only $T = 130$ K with the reduced density $\rho^* = 0.81$ is close to the conditions of low-temperature nonpolar solvents at near-standard conditions when $\rho^* \approx 0.9$ is typically found[62] (the LJ energy for the low-temperature Kr is $\varepsilon_{LJ}/k_B = 180$ K[67]). Therefore, the range of densities available for Kr is not typically accessible by standard solution measurements employing dense molecular solvents.

The PY approximation gives a fair representation of the shape of $S(k)$ for Kr at $T = 130$ K, except for the range of small wavevec-
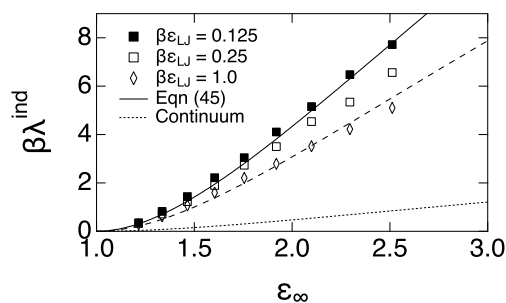

Fig. 4 Induction reorganization energy calculated from simulations changing the solute-solvent induction interaction through the molecular polarizability of the solvent $\alpha^* = \alpha/\sigma_s^3$, $\rho^* = 0.8$. Three sets of points indicate different values of the solvent-solvent LJ interaction energy $\beta\varepsilon_{LJ}$ equal to 0.125 (filled squares), 0.25 (open squares), and 1.0 (open diamonds). The dotted line indicates the reorganization energy in the continuum limit $\tilde{S}(k) \simeq 1$ given by eqn (26) and (38) (cf. to the dotted line in Fig. 2). The approximation $S(k) = \kappa$ leading to eqn (45) is indicated by the solid line ($\kappa = 0.31$) and by the dashed line ($\kappa = 0.22$).

tors where its failure is well documented.[64] This region of k-values does not, however, significantly contribute to λ^{ind}, as we have discussed in relation to Fig. 2. The situation changes, however, when approaching the critical point ($T_c = 209.29$ K and $\rho_c^* = \rho_c\sigma_s^3 = 0.31$ for Kr[66]), as is seen for $S(k)$ at $T = 199$ and 218.18 K. The near-critical spike of $S(k)$ at $k \to 0$ starts to contribute to the k integral in eqn (28), altering the temperature dependence of λ^{ind} (Table 1). Divergence of β_T at the critical point is expected to lead to a spike in λ^{ind} in near-critical fluids. Since the variance of the vertical energy gap is also responsible for inhomogeneous broadening of spectral lines, one can anticipate an enhanced spectral broadening for dyes dissolved in near-critical nonpolar solvents. Note that λ^{ind} scales quadratically with the molecular polarizability of the solvent α. Relatively low values of λ^{ind} in Table 1 compared to those shown in Figs. 2 and 3 for CCl$_4$ are caused by a significantly smaller $\alpha = 2.484$ Å^3 for Kr compared to $\alpha = 11.2$ Å^3 for CCl$_4$.

5 Monte Carlo simulations

We now turn to numerical simulations modeling the redox half reaction in eqn (31). To specify the activation parameters of electron transfer one needs the first and second moments of the stochastic variable V in eqn (32), for which Monte Carlo (MC) simulations[47] are employed here. We consider the case of $z_1 = z = 1$, for which one gets from eqn (33)

$$\langle \Delta F_e \rangle_1 = \langle V \rangle + 2\lambda^{ind}. \tag{46}$$

The reorganization energy is given by eqn (34).

Simulations of the hard-sphere solute in the fluid of LJ molecules were carried out to test the results of the analytical theory. The solvent diameter is taken to be equal to the LJ diameter $\sigma_s = \sigma_{LJ}$ and the simulations were done at the reduced solvent density $\rho^* = \rho\sigma_s^3 = 0.8$. The solvent molecules are excluded from the repulsive hard-sphere core of the solute with the radius a, where $a/\sigma_s = 1$ was adopted in the simulations. The
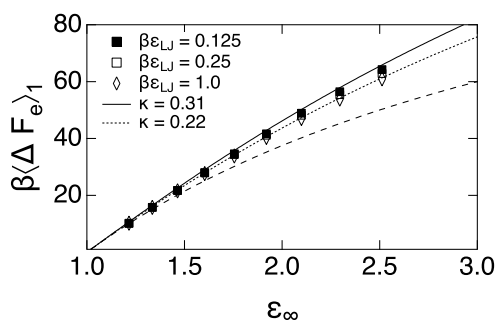
Fig. 5 Average induction-induced shift of the electron-transfer energy gap $\langle \Delta F_e \rangle_1$ vs the high-frequency dielectric constant ε_∞ calculated from the molecular polarizability through the Clausius-Mossotti equation (eqn (27)). Points indicate the results of MC simulation of the hard-sphere solute in fluids of Lennard-Jones (LJ) polarizable spheres with changing molecular polarizability α. Three sets of points indicate different values of the solvent-solvent LJ interaction energy $\beta\varepsilon_{LJ}$ equal to 0.125 (filled squares), 0.25 (open squares), and 1.0 (open diamonds). The dashed line indicates the zero-order in the solute-solvent interaction term $\langle V \rangle$ in eqn (46). The solid line indicates both the full eqn (46) with $\kappa = 0.31$ in eqn (45) used to calculate λ^{ind}. The dotted line refers to the same calculation with $\kappa = 0.22$, which fits λ^{ind} for $\beta\varepsilon_{LJ} = 1.0$ in Fig. 4.

polarizability of the solvent is determined by the reduced polarizability $\alpha^* = \alpha/\sigma_s^3$, which defines the high-frequency dielectric constant of the solvent through the Clausius-Mossotti equation (27). One can thus write the average interaction energy $\langle V \rangle$ for the uncharged solute as follows

$$\langle V \rangle = \frac{3}{2} \frac{\varepsilon_\infty - 1}{\varepsilon_\infty + 2} \frac{e^2}{a}. \tag{47}$$

Similarly, one gets eqn (45) for the reorganization energy. It includes the empirical factor κ accounting for the replacement $S(k) = \kappa$ in eqn (28).

The simulation protocol used to produce the results shown in Figs. 4 and 5 is described in more detail in the ESI.[†] Here, we focus only on the results. Figure 4 shows λ^{ind} calculated from simulations changing α^* in the induction solute-solvent interaction. The solvent polarizability was related to the dielectric constant ε_∞ through the Clausius-Mossotti eqn (27). We found that the same empirical coefficient $\kappa = 0.31$ brings the simulation results for the weakly interacting LJ molecules in agreement with eqn (45) (solid line in Fig. 4), which is consistent to what was found in numerical integration with the PY structure factor of hard-sphere fluids shown in Fig. 2. While density fluctuations of LJ fluids are mostly affected by repulsive interactions between the molecules,[63] increasing the solvent-solvent attraction somewhat modifies the density-density structure factor (Fig. S1 in ESI[†]) and requires a smaller $\kappa = 0.22$ for $\beta\varepsilon_{LJ} = 1.0$ (dotted line in Fig. 4). From simulations, this empirical parameter can be related to the LJ energy by the empirical fit $\kappa = 0.31 - 0.1 \times \beta\varepsilon_{LJ}$. It can be used in combination with LJ energies of molecular solvents tabulated in Ref. 67.

When the parameter κ is used to reproduce the reorganization energies from simulations, the average induction component of the electron-transfer energy gap calculated from eqn (46), (47),

and (45) turns out to be in perfect agreement with simulations (solid and dotted lines in Fig. 5). The dashed line in Fig. 5 shows the zeroth-order perturbation theory (the first term on the right-hand-side of eqn (46) given by eqn (47)). It is insufficient to describe $\langle \Delta F_e \rangle_1$, while the combination of two terms in eqn (46) reproduces simulations.

There is an important distinction between thermodynamics of solvation by dipolar and induction forces. For dipolar solute-solvent interactions V_d, the zeroth-order terms $\langle V_d \rangle$ vanishes because the angular-dependent energy term V_d averages to zero when integrated over the dipolar rotations. Since the term $\langle V_d \rangle$ disappears from the averages, the solvation part of the reaction free energy and the reorganization energy are of the same order of magnitude, and also change with the thermodynamic state in a similar fashion. For instance, the effect of density fluctuations, modifying the reorganization energy, is equally present in the reaction free energy producing the corresponding solvation entropy usually far exceeding the dielectric estimates. For the scalar induction interaction, $\langle V \rangle$ is non-zero and is a dominant contribution to $\langle \Delta F_e \rangle_i$ (Fig. 5). As a result, one gets a substantial separation in magnitudes between $\langle \Delta F_e \rangle_i$ and λ^{ind} (cf. Figs. 4 and 5).

6 Discussion

The derivation performed in Sec. 4 involved one solute sphere as shown in Fig. 1. One can extend this configuration to the reaction of electron transfer in solution when the donor and acceptor particles are represented with spheres carrying the charges z_D and z_A, respectively. One can assign to them the radii R_D and R_A and place them at the distance R_{DA}. The charges change as the result of electron transfer to $z_D + 1$ and $z_A - 1$

$$D(z_D) - A(z_A) \longrightarrow D(z_D + 1) - A(z_A - 1). \tag{48}$$
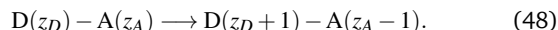
Since the screening of electrostatic interactions between the donor and acceptor by induced dipoles can be neglected for short-ranged induction interactions, eqn (45) transforms to the addition of the donor and acceptor components separately

$$\lambda^{ind} = \frac{3\beta e^4 \sigma_s^3}{320\eta} \kappa \left(\frac{\varepsilon_\infty - 1}{\varepsilon_\infty + 2} \right)^2 \left[\frac{(2z_D + 1)^2}{a_D^5} + \frac{(2z_A - 1)^2}{a_A^5} \right], \tag{49}$$

where $a_{D,A} = R_{D,A} + \sigma_s/2$. For an estimate, for $R_D = R_A$ and a charge-shift reaction, $D - A^+ \rightarrow D^+ - A$, eqn (49) effectively doubles λ^{ind} found for the half reaction. For the configuration with $R_D = R_A = 3$ Å considered in Fig. 2 (CCl$_4$ solvent), one thus anticipates $\lambda^{ind} \simeq 0.2 - 0.3$ eV.

Recent measurements of the rates of electron attachment of solvated electrons to naphthalene in isooctane by Holroyd and Miller[26] produced a large reorganization energy of $\lambda^{ind} \simeq 0.31$ eV. For this reaction, one has $z_D = -1$ and $z_A = 0$ in eqn (48). Further, the relevant solvent parameters are: $\sigma_s = 6.539$ Å,[68] $\varepsilon_\infty = 1.935$, and $\eta = 0.534$. For the naphthalene acceptor ($R_A = 2.665$[69]) its reorganization component in eqn (49) becomes $\lambda_A^{ind} \simeq 0.1$ eV. The total reorganization energy strongly depends on the assigned radius of the solvated electron: assuming that the solvent is expelled from the radius $a_D \simeq 5$ Å (taken from $R_D = R_e \simeq$

1.6 Å to produce the solvent-expelled radius of hydrated electron $a_e \simeq R_e + 1.4 \simeq 3$ Å[70,71]) brings the total $\lambda^{ind} = \lambda_D^{ind} + \lambda_A^{ind}$ to the observable value of 0.31 eV. This calculation assumes that the solvated electron is trapped by the solvent and becomes localized.

For the same configuration of two spherical solutes separated by the distance R_{DA}, the standard Marcus result for the reorganization energy due to dipolar polarization is

$$\lambda^p = e^2 c_0 g^p, \quad g^p = \frac{1}{2R_D} + \frac{1}{2R_A} - \frac{1}{R_{DA}}. \tag{50}$$

This result applies to a solid-like medium described as the dielectric continuum. For molecular polar liquids, both orientational and translational (density) motions of the liquid dipoles become important.[37] These two types of molecular motions separate in the total dipolar reorganization energy $\lambda^p = \lambda^{or} + \lambda^{dens}$ in terms of their distinct dependencies on temperature. The standard Marcus reorganization energy λ^{or} depends on temperature through the liquid density and, therefore, stays constant at constant density. On the contrary, the reorganization energy from dipolar translations gains a hyperbolic temperature dependence, $\lambda^{dens} \propto T^{-1}$, due to the entropic character of the density fluctuations.[13,14,38] Since dipolar and induction interactions carry different symmetries (angular vs scalar) they decouple in the variance and add up in the total solvent reorganization energy

$$\lambda_s = \lambda^{or} + \lambda^{dens} + \lambda^{ind}. \tag{51}$$

The last two summands combine to produce $\lambda^{dens} + \lambda^{ind} \propto T^{-1}$.

There is also an important and potentially observable distinction between λ^p and λ^{ind} in scaling with the solute charge. The dipolar reorganization energy in eqn (50) is proportional to $\Delta z^2 = 1$ and does not depend on the charge state of the reactant. In contrast, for a reduction half reaction, the induction reorganization energy scales as

$$\lambda^{ind} \propto (2z_{Ox} - 1)^2, \tag{52}$$

where $z_{Ox} = z$ is the charge of the oxidized state (eqn (31)). For instance, if λ_1^{ind} characterizes $z = 1 \rightarrow z = 0$ reduction in eqn (31), $9\lambda_1^{ind}$ will apply to $z = 2 \rightarrow z = 1$ and $25\lambda_1^{ind}$ will apply to $z = 3 \rightarrow z = 2$ reactions, respectively.

This result implies that a series of one-electron reduction reactions (such as the multielectron reduction of fullerenes[72,73]) should produce different reorganization energies in each reduction step even if the rest of the solute and solvent parameters remain equal. Correspondingly, a sequence of reduction reactions in a nonpolar solvent should lead to a set of different reorganization energies. Since the induction reorganization energy is always a part of the total solvent reorganization energy, this component will make any chain of sequential electron-transfer reactions depend on the oxidation state. Finally, a strong dependence of the activation barrier on the reactant charge may be a mechanism for kinetically prohibiting reactions characterized by high values of $|z_{Ox}|$.

For non-dipolar solvents, $\lambda^p \rightarrow 0$ and one has to include solvent quadrupoles to describe fluctuations of the polarization density in eqn (5). The dipolar reorganization energy λ^p in eqn (51) is then

replaced with the quadrupolar reorganization energy[30–33] λ^q. In principle, both components are present, but the dipolar part dominates for most polar liquids.

The quadrupolar component of the reorganization energy is given by the following equation[31]

$$\lambda^q = \frac{2\pi e^2}{15} \beta \rho Q^2 \left[\frac{1}{a_D^3} + \frac{1}{a_A^3} \right]. \tag{53}$$

Here, similarly to λ^{ind}, the short-range character of charge-quadrupole interactions leads to $\lambda^q \propto T^{-1}$. The quadrupole scalar Q^2 in eqn (53) is the contraction of the 2-rank tensor $\mathbf{Q}_m$ of the solvent molecular quadrupole calculated relative to the molecular center of mass[52] $Q^2 = (2/3)\mathbf{Q}_m : \mathbf{Q}_m$. The shorter range of charge-quadrupole interactions also produces a stronger, compared to eqn (50), decay of the reorganization energy with the solute size

$$\lambda^q \propto \rho Q^2 a^{-3}. \tag{54}$$

The scaling with the solute size is even stronger for the induction reorganization energy (eqn (45))

$$\lambda^{ind} \propto \rho \alpha^2 a^{-5}. \tag{55}$$

For most molecular materials $\alpha \propto a^3$ when $a \simeq \sigma_s$ and one obtains

$$\lambda^{ind} \propto a^{-2} \tag{56}$$

since the packing density $\eta = (\pi/6)\rho\sigma_s^3$ of the material is constrained by the closest packing of the repulsive cores. Equation (56) produces the scaling of λ^{ind} when the sizes of the solute and the solvent are of close magnitude, $a \simeq \sigma_s$. In contrast to the ground-state polarizability, the polarizability of optically excited semiconductor quantum dots scales with the forth power of their size,[74] $\alpha \propto a^4$. The induction reorganization energy becomes approximately independent of the solute size in that case. This change in the scaling points to the possibility that electronically excited states, such as those used in organic solar cells, can potentially be highly polarizable, thus altering the solvation thermodynamics of induction interactions.

7 Conclusions

We propose that density fluctuations of a nonpolar medium produce thermal fluctuations of the donor-acceptor energy gap to drive charge-transfer reactions with the reorganization energy $\lambda^{ind} \sim 0.1 - 0.3$ eV. Microscopic density fluctuations at the length-scale of the molecular size of the solvent contribute the most to the reorganization energy. The problem thus cannot be reduced to contraction of the solvent cage upon charge transfer described by bulk elastic moduli. The short-range character of the density fluctuations changes the physics of the problem and has an observable consequence in the hyperbolic scaling of the reorganization energy with temperature,

$$\lambda^{ind} \propto T^{-1}. \tag{57}$$

The inverse temperature scaling of the induction reorganization energy applies only to sufficiently small solutes. It loses its

explicit temperature dependence and approaches the limit of the FDT with increasing the solute size. This important macroscopic limit is therefore reached by the formal theory. However, λ^{ind} also drops as the inverse fifth power with increasing the solute size (unless in homogeneous materials with $a \simeq \sigma_s$) and becomes irrelevant in the limit of large solutes. Consequently, in the range of parameters where induction reorganization affects electron transfer, it violates the FDT.

For the donor and acceptor with their sizes comparable to that of the solvent, the hyperbolic temperature scaling of λ^{ind} implies zero activation enthalpy $\Delta H^{\dagger} \simeq 0$ if temperature is altered at constant density (volume). The entire activation barrier becomes entropic, with a negative activation entropy

$$\Delta S^{\dagger}/k_{\text{B}} = -\langle \Delta E \rangle^2/(2\sigma^2) \tag{58}$$

in eqn (1) and (3). Increasing temperature at constant pressure will result in solvent expansion, with both the enthalpic and entropic component of the activation barrier present in the kinetics. However, the dominance of the entropy in the activation barrier is expected to be preserved.

For most practical problems, reorganization energy from classical intramolecular degrees of freedom has to be included; quantum intramolecular vibrations lead to the progression of vibronic transitions included in the corresponding Franck-Condon factor.[75] If λ_i is the internal reorganization energy due to classical intramolecular modes, the overall rate of electron transfer in eqn (1) becomes distinctly non-Arrhenius since the energy-gap variance in eqn (2) becomes

$$\sigma^2 = 2k_{\text{B}}T\lambda_i + (\sigma^{\text{ind}})^2, \tag{59}$$

where $(\sigma^{\text{ind}})^2 = 2k_{\text{B}}T\lambda^{\text{ind}}$ does not carry an explicit dependence on temperature. A linear dependence of σ^2 vs $k_{\text{B}}T$ follows, producing a nonzero intercept equal to $(\sigma^{\text{ind}})^2$. This type of information is accessible from inhomogeneous broadening of optical spectral lines.

The induction component of the vertical energy gap $\langle \Delta F_e \rangle_i$ does not require a specific mode of fluctuations and applies to any polarizable medium. This energy-gap component is substantial in magnitude[76,77] and should be included even for charge transfer in polar liquids where the reorganization energy is dominated by solvent dipoles. In contrast, the induction reorganization energy requires translational motions to be present in the medium. Translations should not only exists to create fluctuations of the donor-acceptor energy gap, but also be sufficiently fast so that many fluctuations could occur on the time-scale of the electron hop. These conditions, typically met for charge transfer in nonpolar molecular liquids, are less applicable to charge transfer in nonpolar solid media, such as organic semiconductors. Local variations of the medium density, which can be viewed as frozen-in density fluctuations, contribute to the energetic disorder affecting charge conductivity.

References

1　Marcus, R. A. Electrostatic free energy and other properties of states having nonequilibrium polarization. I. *J. Chem. Phys.* **24**, 979–989 (1956).

2　Lax, M. The Frank-Condon principle and its application to crystals. *J. Chem. Phys.* **20**, 1752–1760 (1952).

3　Zusman, L. D. Outer-sphere electron transfer in polar solvents. *Chem. Phys.* **49**, 295–304 (1980).

4　Warshel, A. Dynamics of reactions in polar solvents. Semiclassical trajectory studies of electron-transfer and proton-transfer reactions. *J. Phys. Chem.* **86**, 2218–2224 (1982).

5　Nitzan, A. *Chemical Dynamics in Condensed Phases: Relaxation, Transfer and Reactions in Condensed Molecular Systems* (Oxford University Press, Oxford, 2006).

6　Blumberger, J. & Sprik, M. Quantum vs classical electron transfer energy as reaction coordinate for the aqueous Ru^{2+}/Ru^{3+} redox reaction. *Theor. Chem. Acc.* **115**, 113–126 (2006).

7　Kubo, R. The fluctuation-dissipation theorem. *Rep. Prog. Phys.* **29**, 255–284 (1966).

8　Hansen, J.-P. & McDonald, I. R. *Theory of Simple Liquids* (Academic Press, Amsterdam, 2013), 4 edn.

9　Feynman, R. P., Leighton, R. B. & Sands, M. *The Feynman lectures on physics, Vol. I: Mainly mechanics, radiation, and heat* (Addison-Wesley, Reading, MA, 1963).

10　Crisanti, A. & Ritort, F. Violation of the fluctuation–dissipation theorem in glassy systems: basic notions and the numerical evidence. *J. Phys. A: Math. Gen.* **36**, R181–290 (2003).

11　Kurchan, J. In and out of equilibrium. *Nature* **433**, 222–225 (2005).

12　Matyushov, D. V. & Richert, R. Communication: Temperature derivative of the dielectric constant gives access to multipoint correlations in polar liquids. *J. Chem. Phys.* **144**, 041102 (2016).

13　Matyushov, D. V. Energetics of electron transfer reactions in soft condensed media. *Acc. Chem. Res.* **40**, 294–301 (2007).

14　Waskasi, M. M. *et al.* Marcus bell-shaped electron transfer kinetics observed in an Arrhenius plot. *J. Am. Chem. Soc.* **138**, 9251–9257 (2016).

15　Pekar, S. I. Local quantum states of electrons in an ideal ion crystal. *JETP* **16**, 341–348 (1946).

16　Pekar, S. I. *Research in electron theory of crystals* (USAEC, Washington, D.C., 1963).

17　Frölich, H. Electrons in lattice fields. *Adv. Phys.* **3**, 325–361 (1954).

18　Feynman, R. P. Slow electrons in polar crystal. *Phys. Rev.* **97**, 660 (1955).

19　Madden, P. & Kivelson, D. A consistent molecular treatment of dielectric phenomena. *Adv. Chem. Phys.* **56**, 467–566 (1984).

20　Born, M. Volumen und hydratationswärme der ionen. *Z. Phys.* **1**, 45–48 (1920).

21　Matyushov, D. V. Solvent reorganization energy of electron transfer in polar solvents. *J. Chem. Phys.* **120**, 7532–7556

(2004).

22 Lee, S. & Hynes, J. T. Solution reaction path Hamiltonian for reactions in polar solvents. I. Formulation. *J. Chem. Phys.* **88**, 6853–6862 (1988).

23 Matyushov, D. V. Reorganization energy of electron transfer in polar liquids: Dependence on the reactant size, temperature, and pressure. *Chem. Phys.* **174**, 199–218 (1993).

24 Dinpajooh, M., Newton, M. D. & Matyushov, D. V. Free energy functionals for polarization fluctuations: Pekar factor revisited. *J. Chem. Phys.* **146**, 064504 (2017).

25 Benduhn, J. *et al.* Intrinsic non-radiative voltage losses in fullerene-based organic solar cells. *Nat. Energy* **2**, 297–6 (2017).

26 Holroyd, R. A. & Miller, J. R. Rate vs free energy change for attaching highly-mobile electrons to molecules in nonpolar liquids. *J. Phys. Chem. B* **123**, 9206–9211 (2019).

27 Reynolds, L., Gardecki, J. A., Frankland, S. J. V. & Maroncelli, M. Dipole solvation in nondipolar solvents: Experimental studies of reorganization energies and solvation dynamics. *J. Phys. Chem.* **100**, 10337–10354 (1996).

28 Perng, B.-C., Newton, M. D., Raineri, F. O. & Friedman, H. L. Energetics of charge transfer reactions in solvents of dipolar and higher order multipolar character. I. Theory. *J. Chem. Phys.* **104**, 7153–7176 (1996).

29 Perng, B.-C., Newton, M. D., Raineri, F. O. & Friedman, H. L. Energetics of charge transfer reactions in solvents of dipolar and higher order multipolar character. II. Results. *J. Chem. Phys.* **104**, 7177 (1996).

30 Matyushov, D. V. & Voth, G. A. A perturbation theory for solvation thermodynamics: Dipolar-quadrupolar liquids. *J. Chem. Phys.* **111**, 3630 (1999).

31 Milischuk, A. A. & Matyushov, D. V. Equlibrium solvation in quadrupolar solvents. *J. Chem. Phys.* **123**, 044501 (2005).

32 Milischuk, A. A. & Matyushov, D. V. Quadrupolar solvatochromism: 4-amino-phthalimide in toluene. *J. Chem. Phys.* **124**, 204502 (2006).

33 Milischuk, A. A., Matyushov, D. V. & Newton, M. D. Activation entropy of electron transfer reactions. *Chem. Phys.* **324**, 172–194 (2006).

34 Matyushov, D. V. & Schmid, R. Charge separation/recombination reactions in non-polar fluids: a molecular description. *Mol. Phys.* **84**, 533 (1995).

35 Matyushov, D. V. & Schmid, R. Optical and radiationless intramolecular electron transitions in nonpolar fluids: Relative effects of induction and dispersion interactions. *J. Chem. Phys.* **103**, 2034–2049 (1995).

36 Leontyev, I. V. & Tachiya, M. The reorganization energy of electron transfer in nonpolar solvents: Molecular level treatment of the solvent. *J. Chem. Phys.* **123**, 224502 (2005).

37 Bagchi, B. & Chandra, A. Collective orientational relaxation in dense dipolar liquids. *Adv. Chem. Phys.* **80**, 1 (1991).

38 Matyushov, D. V. A molecular theory of electron transfer reactions in polar liquids. *Mol. Phys.* **79**, 795 (1993).

39 Jackson, J. D. *Classical Electrodynamics* (Wiley, New York, 1999).

40 Read, I., Napper, A., Zimmt, M. B. & Waldeck, D. H. Electron transfer in aromatic solvents: The importance of quadrupolar interactions. *J. Phys. Chem. A* **104**, 9385–9394 (2000).

41 Matyushov, D. V. & Ladanyi, B. M. Dispersion solute-solvent coupling in electron transfer reactions. I. Effective potential. *J. Chem. Phys.* **108**, 6362–6377 (1998).

42 Garg, V. *et al.* Conformationally constrained macrocyclic diporphyrin–fullerene artificial photosynthetic reaction center. *J. Am. Chem. Soc.* **133**, 2944–2954 (2011).

43 Lee, M. H., Dunietz, B. D. & Geva, E. Calculation from first principles of intramolecular Golden-Rule rate constants for photo-induced electron transfer in molecular donor–acceptor systems. *J. Phys. Chem. C* **117**, 23391–23401 (2013).

44 Holroyd, R., Miller, J. R., Cook, A. R. & Nishikawa, M. Pressure tuning of electron attachment to benzoquinones in nonpolar fluids: Continuous adjustment of free energy changes. *J. Phys. Chem. B* **118**, 2164–2171 (2014).

45 Zamadar, M. *et al.* Electron transfer by excited benzoquinone anions: Slow rates for two-electron transitions. *J. Phys. Chem. A* **117**, 8360–8367 (2013).

46 Wang, C., Dong, H., Jiang, L. & Hu, W. Organic semiconductor crystals. *Chem. Soc. Rev.* **47**, 422–500 (2018).

47 Allen, M. P. & Tildesley, D. J. *Computer simulation of liquids* (Oxford University Press, Oxford, 1996).

48 Villamaina, D. & Trizac, E. Thinking outside the box: fluctuations and finite size effects. *Eur. J. Phys.* **35**, 035011–21 (2014).

49 Warshel, A. & Parson, W. W. Computer simulations of electron-transfer reactions in solution and in photosynthetic reaction centers. *Annu. Rev. Phys. Chem.* **42**, 279 (1991).

50 Kuharski, R. A. *et al.* Molecular model for aqueous ferrous-ferric electron transfer. *J. Chem. Phys.* **89**, 3248–3257 (1988).

51 Landau, L. D. & Lifshits, E. M. *Statistical physics* (Pergamon Press, New York, 1980).

52 Gray, C. G. & Gubbins, K. E. *Theory of Molecular Liquids* (Clarendon Press, Oxford, 1984).

53 Lazaridis, T. Inhomogeneous Fluid Approach to Solvation Thermodynamics. 1. Theory. *J. Phys. Chem. B* **102**, 3531–3541 (1998).

54 Egorov, S. A. & Skinner, J. L. Vibrational energy relaxation of polyatomic solutes in simple liquids and supercritical fluids. *J. Chem. Phys.* **112**, 275–281 (2000).

55 Lazaridis, T. Solvent reorganization energy and entropy in hydrophobic hydration. *J. Phys. Chem. B* **104**, 4964 (2000).

56 Cao, J., Wu, J. & Yang, S. Calculations of nonlinear spectra of liquid Xe. I. Third-order Raman response. *J. Chem. Phys.* **116**, 3739–3759 (2002).

57 Böttcher, C. J. F. *Theory of Electric Polarization, Vol. 1: Dielectrics in Static Fields* (Elsevier, Amsterdam, 1973).

58 Wertheim, M. S. Exact solution of the mean spherical model for fluids of hard spheres with permanent electric dipole moments. *J. Chem. Phys.* **55**, 4291–4298 (1971).

59 Høye, J. S. & Stell, G. Statistical mechanics of polar systems:

Dielectric constant for dipolar fluids. *J. Chem. Phys.* **61**, 562 (1974).

60 Burke, J. H. & Bird, M. J. Energetics and escape of interchain-delocalized ion pairs in nonpolar media. *Adv. Materials* **31**, 1806863–7 (2019).

61 Prins, P. *et al.* High Intrachain Hole Mobility on Molecular Wires of Ladder-Type Poly(p-Phenylenes). *Phys. Rev. Lett.* **96**, 554–4 (2006).

62 Schmid, R. & Matyushov, D. V. Entropy of attractive forces and molecular nonsphericity in real liquids: A measure of structural ordering. *J. Phys. Chem.* **99**, 2393 (1995).

63 Andersen, H. C., Chandler, D. & Weeks, J. D. Roles of repulsive and attractive forces in liquids: The equilibrium theory of classical fluids. *Adv. Chem. Phys.* **34**, 105–155 (1976).

64 Evans, R. & Schirmacher, W. The long wavelength limit of the liquid structure factor-a theory for the compressibility of liquid rare gases and metals. *J. Physics C: Solid State Physics* **11**, 2437–2451 (1978).

65 Barocchi, F., Chieux, P., Magli, R., Reatto, L. & Tau, M. Static structure of dense krypton and interatomic interaction. *J. Phys.: Condens. Matter* **5**, 4299–4314 (1993).

66 Barocchi, F. *et al.* The pair correlation function of krypton in the critical region: theory and experiment. *J. Phys.: Condens. Matter* **9**, 8849–8871 (1999).

67 Matyushov, D. V. & Schmid, R. Calculation of Lennard-Jones energies of molecular fluids. *J. Chem. Phys.* **104**, 8627–8638 (1996).

68 Ben-Amotz, D. & Herschbach, D. R. Estimation of effective diameters for motecular fluids. *J. Phys. Chem.* **94**, 1038–1047 (1990).

69 Misawa, M. & Fukunaga, T. Structure of liquid benzene and naphthalene studied by pulsed neutron total scattering. *J. Chem. Phys.* **93**, 3495–3502 (1998).

70 Jortner, J. & Noyes, R. M. Some thermodynamic properties of the hydrated electron. *J. Phys. Chem.* **70**, 770–774 (1966).

71 Bartels, D. M. Moment analysis of hydrated electron cluster spectra: Surface or internal states? *J. Chem. Phys.* **115**, 4404–4405 (2001).

72 Reed, C. A. & Bolskar, R. D. Discrete fulleride anions and fullerenium cations. *Chem. Rev.* **100**, 1075–1120 (2000).

73 Sarhangi, S. M., Waskasi, M. M., Hashemianzadeh, S. M. & Matyushov, D. Half reactions with multiple redox states do not follow the standard theory: A computational study of electrochemistry of C_{60} . *J. Phys. Chem. C* **122**, 17080–17087 (2018).

74 Wang, F. *et al.* Exciton polarizability in semiconductor nanocrystals. *Nat. Mater.* **5**, 861–864 (2006).

75 Bixon, M. & Jortner, J. Electron transfer – From isolated molecules to biomolecules. *Adv. Chem. Phys.* **106**, 35–202 (1999).

76 Valeev, E. F., Coropceanu, V., da Silva Filho, D. A., Salman, S. & Brédas, J.-L. Effect of electronic polarization on charge-transport parameters in molecular organic semiconductors. *J. Am. Chem. Soc.* **128**, 9882–9886 (2006).

77 Coropceanu, V. *et al.* Charge transport in organic semiconductors. *Chem. Rev.* **107**, 926–952 (2007).